Journal of Zhejiang University-SCIENCE A (Applied Physics & Engineering)
ISSN 1673-565X (Print); ISSN 1862-1775 (Online)
www.zju.edu.cn/jzus; www.springerlink.com
E-mail: jzus@zju.edu.cn

Optimal velocity functions for car-following models

Milan BATISTA, Elen TWRDY

(*Faculty of Maritime Studies and Transport, University of Ljubljana, 6320 Portorož, Slovenia*)

E-mail: milan.batista@fpp.edu; elen.twrdy@fpp.uni-lj.si

Received June 24, 2009; Revision accepted Nov. 27, 2009; Crosschecked Apr. 30, 2010

Abstract: The integral part of the optimal velocity car-following models is the optimal velocity function (OVF), which can be derived from measured velocity-spacing data. This paper discusses several characteristics of the OVF and presents regression analysis on two classical datasets, the Lincoln and Holland tunnels, with different possible OVFs. The numerical simulation of the formation of traffic congestion is conducted with three different heuristic OVFs, demonstrating that these functions give results similar to those of the famous Bando OVF (Bando *et al.*, 1995). Also an alternative method is present for determining the sensitivity and model parameters based on a single car driving to a fixed barrier.

Key words: Traffic flow, Car following, Optimal velocity function (OVF), Traffic congestion
doi:10.1631/jzus.A0900370 **Document code:** A **CLC number:** U491.1$^+$12

1 Introduction

Car-following theory is focused on the study of single lane traffic with no passing where the driver in each following car is controlled by the car directly in front. For a review and historical development of the subject one should consult (Holland, 1998; Brackstone and McDonald, 2000; Weng and Wu, 2002). Whilst today the study of car-following has practical applications in developing adaptive cruise control systems (Rajamani, 2006), the original theory mostly dealt with the stability analysis of driving with respect to velocity perturbations. The classical result is that instability leads to collision. However, as pointed out by Bando *et al.* (1995), the more likely phenomena resulting from instability is traffic congestion. To demonstrate this idea, Bando *et al.* (1995) proposed the optimal velocity model (OVM) in which the driver's response is proportional to the difference between his optimum speed and his actual speed. The acceleration of a car is thus

$$\frac{\mathrm{d}v_n}{\mathrm{d}t}=\lambda\left(V(h_n)-v_n\right),\quad n=1,2,...,N, \tag{1}$$

where $h_n=x_{n-1}-x_n$ is the distance between the nth car and its predecessor, x_n and $v_n=\dfrac{\mathrm{d}x_n}{\mathrm{d}t}$ are the nth car position and velocity at time t, respectively, λ is the sensitivity of the car-driver system, N is the total number of cars, and $V(h)$ is the optimal velocity function (OVF). They then derived the general stability criterion for the model in Eq. (1):

$$\left.\frac{\mathrm{d}V}{\mathrm{d}h}\right|_{h=h_*}=V'(h_*)<\frac{\lambda}{2}, \tag{2}$$

where h_* is the car spacing of a steady state movement. To illustrate the possibility of spontaneous evaluation of traffic congestion at an unstable condition, Bando *et al.* (1995) took λ=1 and proposed the following OVF:

$$V(h)=\tanh(h-2)+\tanh 2, \tag{3}$$

for which the stability condition is from Eq. (2) and becomes $1-\tanh^2(b-2)<1/2$. This condition divides the domain of OVF into three regions: a stable region near the origin followed by an unstable region,

which is then followed by a stable region at higher velocities. If spacing between cars is such that they are in an unstable region, then a small perturbation in a car's motion will shift it into either neighboring stable region. This mechanism can explain the spontaneous formation of traffic congestion.

Numerous researchers have followed the above idea and they have explored various aspects of the OVM by including delay time (Davis, 2003; Li and Shi, 2006) and/or additional terms in the basic equation. These models include the generalized force model (GFM) proposed by Helbing and Tilch (1998), the full velocity difference model (FVDM) proposed by Jiang *et al.* (2001), the full velocity and acceleration difference model (FVADM) proposed by Zhao and Gao (2006), the total generalized optimal velocity model (TGOVM) proposed by Zhu and Liu (2008) and the recently proposed Wilson model (Wilson, 2008), which generalizes OVM with relative velocity and optimal headway terms. In the literature one can also find OVF which differs from Bando's OVF in Eq. (3). Among them are piece-wise linear OVF (Nakanishi *et al.*, 1997), hyperbolic OVF (Batista, 2000; Gasser *et al.*, 2004; Orosz *et al.*, 2004; 2005), and a modified form of OVF (Eq. (3)) having more parameters (Tadaki *et al.*, 1999) with values that can be determined from observed traffic flow data.

The main objective of this paper is to systematically investigate possible choices of the OVF which can be related to empirical data and which possess the same properties as Eq. (3) and lead to a similar traffic phenomena. In addition, an alternative way to determine the sensitivity parameter in Eq. (1) is discussed.

2 Suitable optimal velocity functions

Since the car-following theory is a mixed social-physical theory, one cannot expect that any natural OVF exists. The selection of the OVF thus depends on a user's choice. However, this choice cannot be completely arbitrary since the OVF must satisfy several analytical conditions to describe the observed relation between spacing and velocity. The following are the most noticeable observed properties of the OVF (Del Castillo and Benitez, 1995a):

1. There is a safety distance h_0 between car stops.
2. The speed of the car increases with increased spacing.
3. There is a free flow speed; i.e., the speed of a car travelling alone.

The analytical conditions which could be derived from the above requirements are as follows (Bando *et al.*, 1995; Gasser *et al.*, 2004; Orosz *et al.*, 2004):

1. The OVF should be a continuous non-negative function defined for $h\geq 0$.
2. The OVF should be a monotone (Bando *et al.*, 1995); i.e., $V'(h)\geq 0$ for $h\geq 0$.
3. The OVF should have a lower limit boundary; i.e., for some $h_0\geq 0$ the car should stop, so $V(h)=0$ for $h\leq h_0$.
4. The OVF should have a upper limit boundary (Bando *et al.*, 1995); i.e., $v_{\max}=\lim_{h\to\infty}V(h)$.

To ensure that the OVF will predict the formation of a state of congestion one should also demand that the derivative of the OVF should be concave (bell-like), so it has three possible consecutive regions: stable→unstable→stable (Gasser *et al.*, 2004).

This property will be satisfied if the first derivative of the OVF is a continuous function and has a single maximum for some $h_m>h_0>0$, or if the first derivative of the OVF is a piecewise continuous monotonically decreasing function with discontinuity at $h_m>h_0>0$ where it has the maximum value. On the basis of Eq. (2) one can define the maximum of the derivative of the OVF as the threshold sensitivity.

$$\lambda_m \equiv 2\max_{h\geq h_0} V'(h), \tag{4}$$

below which the motion may become unstable. When the first derivative of the OVF is a continuous function, its local maximum is determined by $V''(h_m)=0$. In this case, the OVF has an inflection point at h_m, hence this distance will be called the 'inflection distance' regardless of the possibility that h_m is the point of discontinuity of $V'(h)$. To these, one can also add some user oriented properties:

1. The OVF should be simple mathematically.
2. If possible, a single function should represent the whole range of spacing.

Now, the question arises as to whether one can determine the appropriate OVF from the listed properties. Obviously, the polynomial form of the OVF cannot ensure the existence of the free flow speed, so

the next simplest function for a possible OVF is the rational function:

$$V(h)=\frac{a_0+a_1h+...+a_mh^m}{b_0+b_1h+...+b_nh^n}, \tag{5}$$

where m and n are integers. The condition $V(h_0)=0$ is fulfilled by taking $h_0=0$ and $a_0=0$, and the condition $v_{\max}=\lim_{h\to\infty}V(h)$ is satisfied by setting $n=m$ and $a_n=v_{\max}b_n$. In this way the OVF in Eq. (5) can transform into

$$\begin{aligned}V(h)&=\frac{a_1h+a_2h...+a_nh^n}{b_0+b_1h+...+b_nh^n}\\&=v_{\max}\frac{h(h^{n-1}+\alpha_{n-2}h^{n-2}+...+\alpha_1h+\alpha_0)}{h^n+\beta_{n-1}h^{n-1}+...+\beta_1h+\beta_0}.\end{aligned} \tag{6}$$

Furthermore, to ensure that $V(h)\geq 0$, all the polynomial coefficients should be non-negative $\alpha_k, \beta_k\geq 0$, and the simplest way to ensure that $V'(h)\geq 0$ is to set $\alpha_k=0$, for $k=0, 1, \ldots, n-2$. Thus, the desired OVF takes the form as

$$V(h)=v_{\max}\frac{h^n}{h^n+\beta_{n-1}h^{n-1}+...+\beta_1h+\beta_0}. \tag{7}$$

Now, the derivative of the OVF should have a single extreme, so the equation $V''(h)=0$ should give only one, possibly multiple, solution for $h>0$. Performing the required derivatives, one can conclude that the simplest way to obtain the desired result is that $\beta_k=0$, $k=1, 2, \ldots, n-1$, so the solution of $V''(h)=0$ is $h_m=\sqrt[n]{\beta_0(n-1)/(n+1)}$. From this, when $n>1$, one can express $\beta_0=h_m^n(n+1)/(n-1)$. Thus, the final form of the desired OVF is

$$V(h)=v_{\max}\frac{h^n}{h^n+h_m^n(n+1)/(n-1)},\quad n>1. \tag{8}$$

This function will be called the 'hyperbolic OVF'.

In Table 1, several other functions which meet the above demands are listed. The Greenshields-

Table 1 Various optimal velocity functions (OVFs)

OVF	$V(h)$	$v_{\max}=\lim_{h\to\infty}V(h)$	h_m	h_0
Bando (Bando *et al.*, 1995)	$a\left(\tanh\frac{h-h_m}{b}+\tanh\frac{h_m}{b}\right)$	$a\left(1+\tanh\frac{h_m}{b}\right)$	–	0
Trigonometric	$a\left(\arctan\frac{h-h_m}{b}+\arctan\frac{h_m}{b}\right)$	$a\left(\frac{\pi}{2}+\arctan\frac{h_m}{b}\right)$	–	0
Hyperbolic (Batista, 2000; Gasser and Werner 2004; Orosz *et al.*, 2004; 2005)	$\begin{cases}0, & h\leq h_0,\\ v_{\max}\frac{(h-h_0)^n}{b^n+(h-h_0)^n}, & h>h_0\end{cases}$	–	$h_0+b\sqrt[n]{\frac{n-1}{n+1}}$, $n\geq 1$	–
Greenshields-based (May, 1990; Castillo and Benitez, 1995)	$\begin{cases}0, & h\leq h_0,\\ v_{\max}\left(1-(h_0/h)^n\right)^m, & h>h_0\end{cases}$	–	$h_0\left(\frac{n+1}{mn+1}\right)^{-\frac{1}{n}}$	–
Underwood (May, 1990; Castillo and Benitez, 1995)	$v_{\max}\exp\left(\frac{-2h_m}{h}\right)$	–	–	0
Newell-based (Edie, 1961)	$\begin{cases}0, & h\leq h_0,\\ v_{\max}\left(1-\exp\left(-\left(\frac{h-h_0}{b}\right)^n\right)\right), & h>h_0\end{cases}$	–	$h_0+b\sqrt[n]{\frac{n-1}{n}}$, $n\geq 1$	–
Kerner-Konhauser (Kerner and Konhauser, 1993)	$\begin{cases}0, & h\leq h_0,\\ a\left(\left(1+\exp\left(\frac{b}{h}-c\right)\right)^{-1}-d\right), & h>h_0\end{cases}$	$a\left(\frac{1}{1+\mathrm{e}^{-c}}-d\right)$	Numeric	$\frac{b}{c+\ln\left(\frac{1}{d}-1\right)}$

a, b, c, d, and n are function parameters without definite physical meanings

based, the Underwood, the Newell-based, and the Kerner-Konhauser OVFs are established from speed-density models by replacing traffic density k with spacing h=1/k. Several comments about these functions are justified. First, the Greenshields OVF can be classified according to the values of parameters m and n (May, 1990) to the original Greenshields OVF when m=n=1, the Drew OVF when m=1 and the Pipes OVF when n=1. Also in the original Newell OVF n=1. Next, note that v_{max} is the parameter for the hyperbolic, the Greenshields, the Underwood, and the Newell OVFs. For others functions it is calculated. If possible the stopping distance h_0 is used as a parameter, otherwise the inflection distance h_m is used. As such the inflection distance is a mathematical future of an OVF, but it also has some physical meaning. Namely, it represents the distance between cars where one may expect instabilities in flow. The inflection distance is thus used as a parameter for the Bando, the trigonometric, and the Underwood OVFs, while the stopping distance h_0 is the parameter for the hyperbolic, the Greenshields-based, and the Newell-based OVFs. For the latter functions the inflection distance is calculated. Note that in the case h_0=0, the hyperbolic and Newell OVFs will have the inflection point only for n>1. Also note that the inflection distance of the Kerner-Konhauser OVF must be calculated numerically.

3 Regression analysis of experimental data

To judge the quality of the proposed OVF, a regression analysis of the experimental data of measured speed and distance on single line traffic was undertaken. One dataset is taken from Edie (1961) where measurement was carried out in the Lincoln tunnel (New York, USA) and contains a 1643-vehicle sample, and the other dataset is taken from Rothery (1997) where measurement was carried out in the Holland tunnel (New York, USA) and contains a 23 377-vehicle sample. Here, it must be emphasized that these classical datasets are used because they are generally accessible. Each data point is taken into regression analysis assuming that they correspond to equilibrium conditions (Del Castillo and Benitez, 1995b). Results of the regression analysis are shown in Table 2, and the resulting OVFs are shown in Fig. 1.

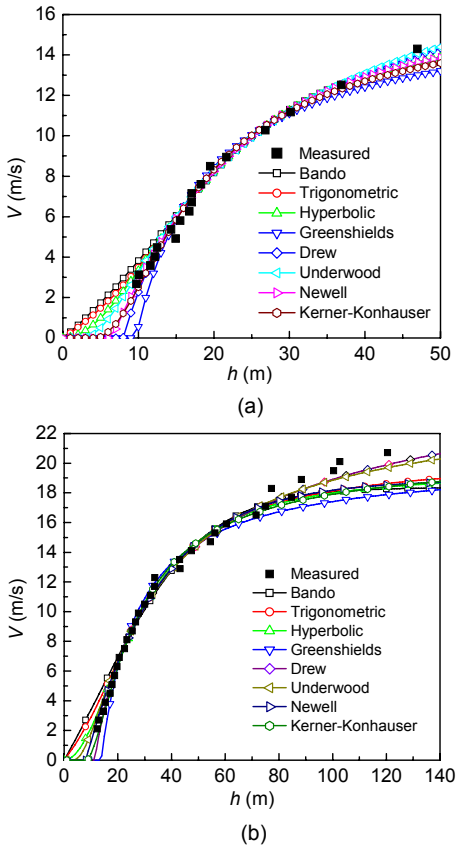

Fig. 1 Various optimal velocity functions for datasets of (a) Lincoln tunnel and (b) Holland tunnel

Considering the obtained results, one can see that all the models are well described using experimental data with a correlation coefficient (R^2) above 0.95 and also that narrow confidence intervals for the best-fit parameters values are obtained. In the case of the Lincoln tunnel dataset, the Bando OVF gives the lowest limit speed 14.04 m/s, while the highest, 31 m/s, is given by the Drew OVF. The smallest inflection distance, 6.5 m, is predicated by the Newell OVF and the highest, 14.0 m, by the trigonometric OVF. Similar observations were hold for the Holland tunnel dataset. The Bando OVF gives the lower final speed, 18.7 m/s, and the Drew OVF gives the highest final speed, 33 m/s. Also the smallest inflection distance, 8.1 m, is given by the Newell OVF and the largest, 18.8 m, is given by the trigonometric OVF. For both datasets the stopping distance in the hyperbolic OVF was fixed at zero because otherwise the exponent n obtained by regression would be less than one. The analysis suggests that there is no theoretical argument for selecting any of the proposed functions

Table 2 Results of the velocity-spacing regression analysis for various OVFs

Dataset	OVF	v_{max} (m/s)	h_m (m)	h_0 (m)	a (m/s)	b (m)	c	d	n	R^2	λ_m (s^{-1})
Lincoln tunnel	Bando	14.04*	12.78±0.17		8.97±0.12	20.01±0.36				0.974	0.90*
	TG	16.07*	13.96±0.06		6.79±0.07	13.67±0.23				0.979	0.99*
	HB	15.57±0.10	11.53*	0**		18.94±0.13			2.09±0.02	0.981	1.09*
	GS	16.38±0.03	9.66±0.02	9.66±0.02						0.968	3.39*
	Drew	31.32±0.98	7.98±0.06	7.98±0.06					0.33±0.01	0.986	2.62*
	Pipes	19.06±0.10	9.73*	4.90±0.21					2.97±0.16	0.985	1.47*
	UW	20.93±0.06	9.35±0.03							0.983	1.21*
	MNW	17.81±0.39	8.49±0.13	8.49±0.13		21.74±1.03			0.74±0.02	0.985	∞*
	NW	15.03±0.07	6.50±0.08	6.50±0.08		17.0±0.023			1**	0.983	1.77
	KK	16.91	10.87*	4.73	24.29	29.63	0.850	0.00440		0.984	1.40*
Holland tunnel	Bando	18.67*	12.71±0.16		14.01±0.07	39.39±0.19				0.977	0.71*
	TG	20.76*	18.79±0.05		9.26±0.02	23.70±0.09				0.984	0.78*
	HB	20.09±0.03	14.76*	0**		29.17±0.05			1.86±0.00	0.986	0.87*
	GS	20.22±0.01	13.84±0.01	13.84±0.01						0.971	2.92*
	Drew	33.04±0.13	11.33±0.02	11.33±0.02					0.39±0.00	0.992	2.27*
	Pipes	23.03±0.02	13.65*	6.00±0.07					3.55±0.05	0.991	1.20*
	UW	24.40±0.01	12.92±0.01							0.989	0.88*
	MNW	21.69±0.05	12.07±0.03	12.07±0.03		32.79±0.20			0.71±0.00	0.991	∞*
	NW	18.86±0.02	8.09±0.03	8.09±0.03		27.69±0.08			1**	0.987	1.36
	KK	20.80	15.30*	8.81	30.84	41.49	0.822	0.02012		0.987	1.25*

* Calculated; ** Assumed; Bando: Bando *et al*. (1995); TG: trigonometric; HB: hyperbolic; GS: Greenshield; UW: Underwood; MNW: modified Newell; NW: Newell; KK: Kerner-Konhauser

except the practical one of choosing that with the simplest mathematical structure.

4 Heuristic OVF models

In this section, the heuristic hyperbolic, the Underwood, and the Newell OVFs, which are alternatives to the Bando OVF in Eq. (3), will be considered. In order that the proposed functions will be in some way comparable with Eq. (3) note that the Bando OVF function incorporates the following traffic characteristics:

$$h_0 = 0,\quad h_m = 2,\ v_{\max} = 1 + \tanh 2 \approx 2,\ \lambda_m = 2. \quad (9)$$

From Table 1 one can see that in the hyperbolic and Newell OVFs, the inflection distance h_m is determined by model parameter b and exponent n, so one of them must be chosen. However, to keep the models simple we relax the condition h_m=2 and choose b and n as integers. Thus, the proposed heuristic hyperbolic OVF is

$$V = \frac{2h^4}{16 + h^4},\quad h_m = 2\sqrt[4]{3/5} \approx 1.76,\ \lambda_m \approx 2.13. \quad (10)$$

And the proposed Newell OVF is

$$V = 2(1 - \mathrm{e}^{-h^4/16}),\ h_m = \sqrt[4]{12} \approx 1.86,\ \lambda_m \approx 3.10. \quad (11)$$

Using Eq. (9) and the formulas in Table 1, one can immediately establish the Underwood OVF in the form of $V = 2\mathrm{e}^{-4/h}$. However, this function has a very gentle rise and a low threshold sensitivity due to the condition v_{max}=2. To obtain a simple function which is close to Eq. (3) in the unstable region, the maximal velocity should rise to v_{max}=5, so the Underwood OVF becomes

$$V = 5\mathrm{e}^{-4/h},\ h_m = \sqrt[4]{12} \approx 1.86,\ \lambda_m \approx 1.35. \quad (12)$$

From the above, one can see that the closest to Eq. (9) is the hyperbolic OVF in Eq. (10). This can also be observed from Fig. 2 where the proposed heuristic OVFs together with their first derivative are shown.

5 Numerical simulation of traffic congestion

In this section, the heuristic OVFs and data-fitted OVFs are used for numerical simulation of traffic congestion on a circular road.

Firstly, the simulation using the proposed heuristic OVFs for N=100 identical cars with λ=1 moving on the circuit of length L=200 was conducted. The steady state distance between cars is h_*=2, so in Fig. 2b the cars are in the unstable region for all the OVFs. The results of the simulation are shown in Fig. 3 where the time evaluation of traffic congestion in x-t space for various models is displayed. As can be observed, all the four models predict the formation of clusters, but they differ in the clusters numbers. Both the Bando and hyperbolic OVFs forms five clusters, the Newell and Underwood OVFs forms three and two clusters, respectively. Note also that the appearances of the evaluations of congestion are similar to that of the Bando and hyperbolic OVFs. This was expected since both the OVFs have similar traffic flow characteristics.

We do not know of any theory in which the exact number of clusters can be predicted for a particular OVF. However, as is known from linear stability analysis of OVMs the stability boundary of the steady state flow is given by Bando *et al.* (1995).

$$V'(h_*)=\frac{\lambda}{2\cos^2(k\pi/N)},\quad k=0,1,...,N/2, \quad (13)$$

where k is the so-called wave number. In the considered case $V'(h_*)$ has the values of 0.68, 1.00, 1.07, and 1.47 for the Underwood, Bando, hyperbolic, and Newell OVFs, respectively. One can thus expect that the number of clusters will be the lowest for the Underwood OVF and the highest for the Newell OVF. However, for the Newell OVF this is not the case.

The second simulation is conducted for an OVM using the Bando, hyperbolic, Underwood, and Newell

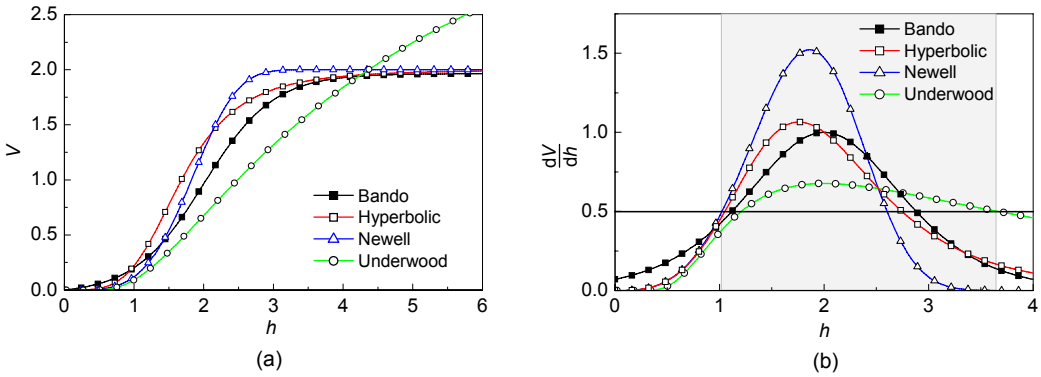

Fig. 2 Heuristic optimal velocity functions (a) and the first derivative of optimal velocity functions (b)
The shaded region in Fig. 2b indicates the union of OVF's unstable region for λ=1

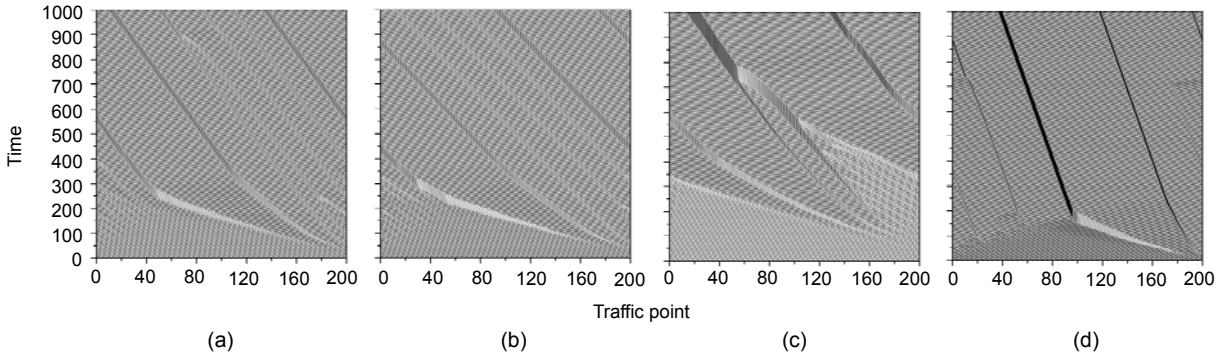

Fig. 3 Simulation of traffic congestion with 100 cars on a circular road of length 200 for λ=1 with different optimal velocity functions
(a) Bando OVF; (b) Hyperbolic OVF; (c) Underwood OVF; (d) Newell OVF

OVFs and data-fitted for the Lincoln tunnel (Table 2). Fig. 4 shows the first derivation of these OVFs, where a similarity of the hyperbolic and the Underwood curves can be observed. Also note that for the Newel OVF, the stopping distance presents a barrier with infinite sensitivity. Thus, unlike other OVFs, for the Newel OVF there exists an unstable region for any sensitivities. In Fig. 5, the simulation dynamic evaluation of traffic congestion for N=100 identical cars moving on the circuit of length L=1200 m for different OVFs with λ=0.8 is presented. Moreover, it can be observed that the number of formed clusters depends on the model used. In the case of the hyperbolic, Underwood, and the Newell models, four, five, and two clusters are formed in about 0.5 h, respectively. For the Bando model five somewhat inexpressive clusters are formed in about 1.5 h.

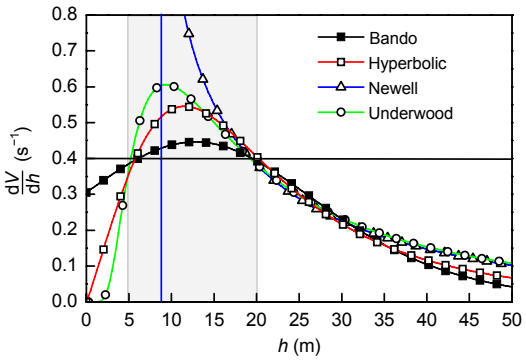

Fig. 4 The first derivative of various OVFs using data for the Lincoln tunnel. The shaded region indicates the union of the OVF's unstable regions for λ=0.8

6 Alternative determination of the sensitivity and the model's parameters

While the OVF is essentially a static property of the traffic flow, the sensitivity is not. In this section the alternative method of the determination of sensitivity will be given. In general, a car-following model of traffic flow is a set of differential Eq. (1), each describing the motion of a single car in a line. In the special case when there are only two cars, and the front car is at the distance $x_{n-1}=L$ from the tailing car and does not move; i.e., $v_{n-1}=0$, then Eq. (1) is reduced to a system of two equations.

$$\frac{\mathrm{d}v}{\mathrm{d}t}=\lambda\big(V(L-x)-v\big),\quad \frac{\mathrm{d}x}{\mathrm{d}t}=v. \tag{14}$$

The solution of this equation with the initial conditions $x(0)=v(0)=0$ describes a car driving from a state of rest ahead to a fixed barrier. Comparing the solution with experimental data, one can estimate the sensitivity λ and the parameters included in the particular OVF used.

To confirm the idea, several runs to a fixed barrier at a distance of 53 m was undertaken, where the acceleration, velocity and distance were recorded using a Vericom VC3000 dynamometer (Vericom Computers Inc., USA). The mean measured velocities were then compared with the calculated velocities

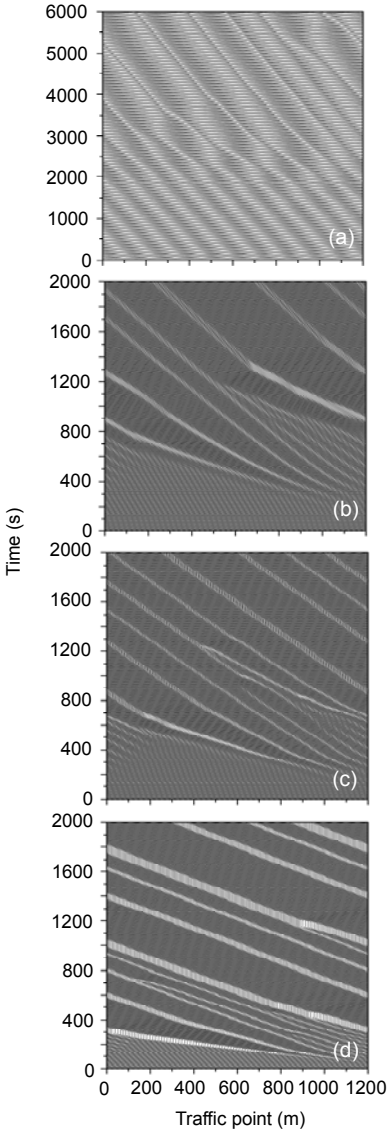

Fig. 5 Simulation of traffic congestion with 100 cars on a circular road of length 1200 m for λ=0.8 for (a) Bando OVF, (b) Hyperbolic OVF, (c) Underwood OVF, and (d) Newell OVF using data for the Lincoln tunnel

using three different OVFs: the hyperbolic with n=2, the Greenshields, and the Underwood. These OVFs were selected for a computational reason. All require just two function parameters to be determined. The sensitivity and the particular OVF's parameters were calculated by minimizing the sum of squares of difference between the measured and the calculated velocities. The results of this calculation are shown in Table 2, and the corresponding acceleration, velocity, and distance curves are shown in Fig. 6. As seen from these figures, all three OVFs predict relatively high initial acceleration, which is above the physical limit of single axes driven cars, and also all three models overshoot the barrier distance. Note that the drop in acceleration that may be observed (measured) is the result of shifting gears from the first to the second (this drop may of course be eliminated using a car with an automatic transmission). The estimated sensitivity of models is between 0.5 and 0.7 s^{-1}. These values are comparable to those obtained by Chandler *et al.*, who performed the experiment with two wire-connected cars (Rothery, 1997) and reported the sensitivity between 0.17 and 0.74 s^{-1}. Also the present sensitivities are comparable to those obtained by Kesting and Treiber (2009) which were Calibrating OVM with real traffic data and reported values between 0.67 and 0.80 s^{-1} (Table 1, OVM, relative error measure). Using data in Table 3, one may approximately estimate that the unstable car's spacing for the hyperbolic OVF is 4–13 m, the Greenshields OVF 11–27 m, and the distances for the Greenshields and the Underwood OVFs are comparable to the inflection distances for Underwood OVF 5–20 m. Note that the inflection obtained by regression analysis of the Lincoln tunnel dataset is within 10% (Table 2).

Since the initial acceleration predicted by the models is too high, the basic model in Eq. (1) was modified so that the acceleration limited by friction (Daganzo, 2003) was taken into account. The proposed modified model is

$$\frac{\mathrm{d}v}{\mathrm{d}t}=\max\left(a_{\max},\lambda(V-v)\right). \tag{15}$$

The resulting sensitivity and the model parameters determined by minimizing the sum of squares of difference between the measured and calculated velocities by Eq. (15) are shown in Table 3. It can be seen that the sensitivity of the modified OVM increase to 1.1–1.5 s^{-1}. Consequently, the unstable spacing as compared to the non-modified model is narrower. For the hyperbolic OVF, the unstable

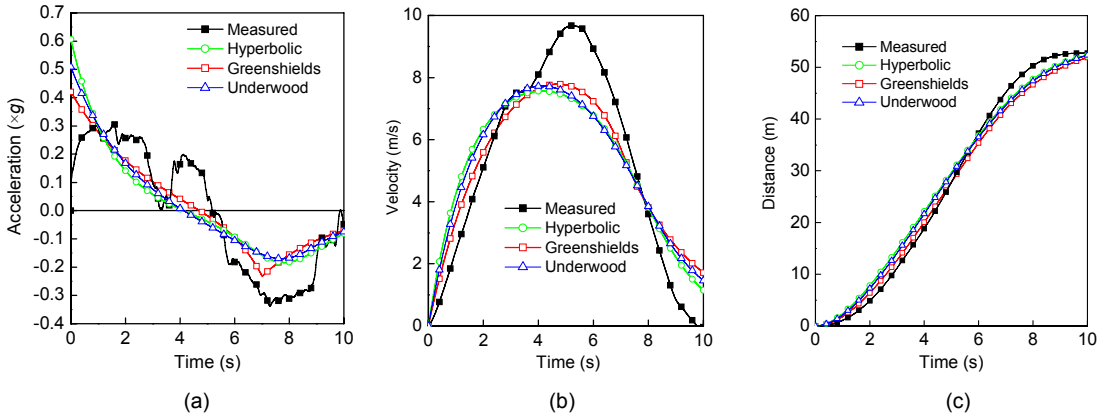

Fig. 6 Measured and calculated kinematical variables for different OVFs (driving on to the fixed barrier)
(a) Acceleration; (b) Velocity; (c) Distance

Table 3 Estimated values of parameters for different OVFs (driving on to the fixed barrier)

OVF	OVM				Modified OVM			
	λ (s^{-1})	$v_{\max}$ (m/s)	h_m (m)	SD_v (m/s)	λ (s^{-1})	$v_{\max}$ (m/s)	h_m (m)	SD_v (m/s)
Hyperbolic	0.7	9	7.5	1.40	1.5	9	4.0	0.69
Greenshields	0.4	13	11.0	1.20	1.2	10	4.0	0.72
Underwood	0.5	14	9.0	1.34	1.1	11	4.0	0.82

spacing is 3–6 m, the Greenshields OVF 4–8 m, and the Underwood OVF 1–7 m. As can be seen from Fig. 7, the acceleration, velocity, and the distance curves better follow the measured values and notably the predicted barrier distance is not overshot.

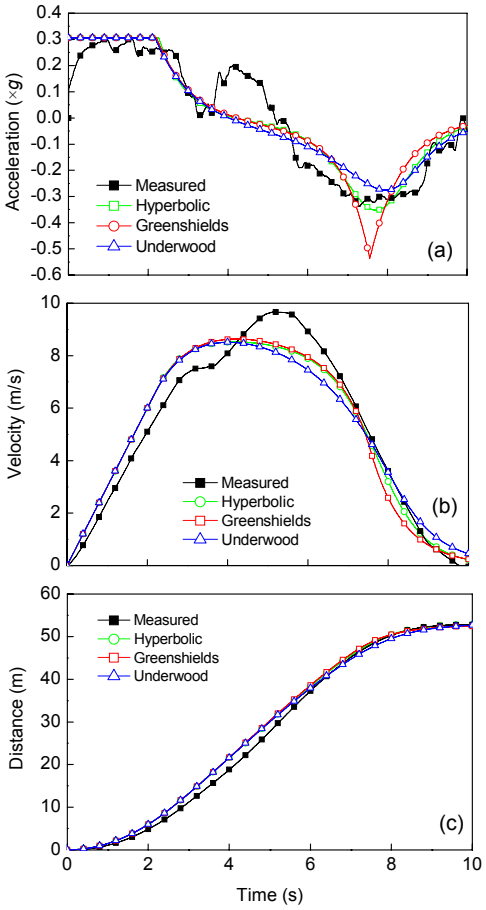

Fig. 7 Measured and calculated kinematical variables for different modified OVFs using a modified OVM (driving on to a fixed barrier)
(a) Acceleration; (b) Velocity; (c) Distance

7 Conclusions

The results of the present study can be summarized as follows. Firstly, it was shown that the OVF may be characterized by final velocity, stopping distance, and inflection distance. These data can be obtained from measured, velocity- spacing traffic data by regression analysis. None of the discussed OVFs was confirmed as the best possible choice since all yield similar results. Secondly, it was also demonstrated that OVFs that confirm the analytical requirements stated in the second section predict phenomena similar to the original Bando *et al*. (1995) model. However, they differ regarding position and length of unstable spacing region, threshold sensitivity, and the number of clusters formatted. Thirdly, an alternative method of obtaining the sensitivity parameter was presented based on the analysis of data obtained by driving a single car to a fixed barrier. The obtained sensitivities are comparable to those obtained by other researches.

References

Bando, M., Hasabe, K., Nakayama, A., Shibata, A., Sugiyama, Y., 1995. Dynamical model of traffic congestion and numerical simulation. *Physical Review E*, **51**(2):1035-1042. [doi:10.1103/PhysRevE.51.1035]

Batista, M., 2000. Numerical Simulation of Traffic Congestion. International Conference on Traffic Science. Portorož, Slovenia, p.361-367.

Brackstone, M., McDonald, M., 2000. Car following: a historical review. *Transportation Research Part F*, **2**(4):181-196. [doi:10.1016/S1369-8478(00)00005-X]

Daganzo, C.F., 2003. Fundamentals of Transportation and Traffic Operations. Science Ltd., USA.

Davis, L.C., 2003. Modifications of the optimal velocity traffic model to include delay due to driver reaction time. *Physica A: Statistical Mechanics and its Applications*, **319**(1):557-567. [doi:10.1016/S0378-4371(02)01457-7]

Del Castillo, J.M., Benitez, F.G., 1995a. On the functional form of the speed-density relationship—I: general theory. *Transportation Research Part B: Methodological*, **29**(5):373-389. [doi:10.1016/0191-2615(95)00008-2]

Del Castillo, J.M., Benitez, F.G., 1995b. On the functional form of the speed-density relationship—II: empirical investigation. *Transportation Research Part B: Methodological*, **29**(5):391-406. [doi:10.1016/0191-2615(95)00009-3]

Edie, L.C., 1961. Car-following and steadystate theory for noncongested traffic. *Operations Research*, **9**(1):66-76. [doi:10.1287/opre.9.1.66]

Gasser, S.G., Werner, B., 2004. Bifurcation analysis of a class of 'car following' traffic models. *Physica D: Nonlinear Phenomena*, **197**(3-4): 222-241. [doi:10.1016/j.physd.2004.07.008]

Helbing, D., Tilch, B., 1998. Generalized force model of traffic dynamics. *Physical Review E*, **58**(1):133-138. [doi:10.1103/PhysRevE.58.133]

Holland, E.N., 1998. A generalized stability criterion for motorway traffic. *Transportation Research Part B: Methodological*, **32**(1):141-154. [doi:10.1103/PhysRevE.58.133]

Jiang, R., Wu, Q., Zhu, Z., 2001. Full velocity difference model for car-following theory. *Physical Review E*, **64**(1):017101. [doi:10.1103/PhysRevE.64.017101]

Kerner, B.S., Konhauser, P., 1993. Cluster effect in initially

homogeneous traffic flow. *Physical Review E*, **48**(4):R2335-R2338. [doi:10.1103/PhysRevE.48.R2335]

Kesting, A., Treiber, M., 2009. Calibration of Car-following Models Using Floating Car Data. *In*: Traffic and Granular Flow'07. Springer, Berlin, Germany. [doi:10.1007/978-3-540-77074-9_10]

Li, L., Shi, P., 2006. Numerical analysis on car-following traffic flow models with Delay Time. *Journal of Zhejiang University-SCIENCE A*, **7**(2):204-209. [doi:10.1631/jzus.2006.A0204]

May, A.D., 1990. Traffic Flow Fundamentals. Prentice-Hall, New York, USA.

Nakanishi, K., Itoh, K., Igarashi, Y., Bando, M., 1997. Solvable optimal velocity models and asymptotic trajectory. *Physical Review E*, **55**(6):6519-6532. [doi:10.1103/PhysRevE.55.6519]

Newell, G.F., 1961. Nonlinear effects in the dynamics of car following. *Operations Research*, **9**(2):209-229. [doi:10.1287/opre.9.2.209]

Orosz, G., Wilson, R.E., Krauskopf, B., 2004. Global bifurcation investigation of an optimal velocity traffic model with driver reaction time. *Physical Review E*, **70**(2):026207. [doi:10.1103/PhysRevE.70.026207]

Orosz, G., Krauskopf, B., Wilson, R.E., 2005. Bifurcations and multiple traffic jams in a car-following model with reaction-time delay. *Physica D: Nonlinear Phenomena*, **211**(3-4):277-293. [doi:10.1016/j.physd.2005.09.004]

Rajamani, R., 2006. Vehicle Dynamics and Control. Springer, New York, USA.

Rothery, R.W., 1997. Car Following Models. *In*: Monograph on Traffic Flow Theory. Available from http://www.tfhrc.gov/its/tft/tft.htm.

Tadaki, S., Kikuchi, M., Sugiyama, Y., Yukawa, S., 1999. Noise induced congested traffic flow in coupled map optimal velocity model. *Journal of Physical Society of Japan*, **68**(9):3110-3114. [doi:10.1143/JPSJ.68.3110]

Weng, Y., Wu, T., 2002. Car-following models of vehicular traffic. *Journal of Zhejiang University-SCIENCE A*, **3**(4):412-417. [doi:10.1631/jzus.2002.0412]

Wilson, R.E., 2008. Mechanisms for spatio-temporal pattern formation in highway traffc models. *Philosophical Transactions of the Royal Society A: Mathematical Physical and Engineering Sciences*, **366**:2017-2032. [doi:10.1098/rsta.2008.0018]

Zhao, X., Gao, Z., 2005. A new car-following model: full velocity and acceleration difference model. *The European Physical Journal B*, **47**(1):145-150. [doi:10.1140/epjb/e2005-00304-3]

Zhu, W., Liu, Y., 2008. A total generalized optimal velocity model and its numerical tests. *Journal of Shanghai Jiaotong University (Science)*, **13**(2):166-170. [doi:10.1007/s12204-008-0166-9]